

1 **Rapidly increasing sulfate concentration: a hidden promoter of eutrophication in**
2 **shallow lakes**

3 Chuanqiao Zhou^{a,1}, Yu Peng^{a,1}, Li Chen^a, Miaotong Yu^a, Muchun Zhou^b, Runze Xu^a,
4 Lanqing Zhang^a, Siyuan Zhang^c, Xiaoguang Xu^{a,*}, Limin Zhang^a, Guoxiang Wang^a

5 ^a School of Environment, Nanjing Normal University, Jiangsu Center for Collaborative
6 Innovation in Geographical Information Resource Development and Application,
7 Jiangsu Key Laboratory of Environmental Change and Ecological Construction,
8 Nanjing 210023, China

9 ^b China Aerospace Science and Industry Nanjing Chenguang group, Nanjing 210022,
10 China

11 ^c School of Energy and Environment, Southeast University, Nanjing 210096, China

12 **Corresponding author: 1, Wenyuan Road, Xianlin University District, Nanjing,*
13 *210023, China*

14 *E-mail address: xxg05504118@163.com*

15 ¹ Both authors contributed equally

16 **Keywords:** Sulfate reduction; iron reduction; phosphorus release; eutrophication;
17 sulfate reduction bacteria

18 **Abstract:**

19 Except for excessive nutrient input and climate warming, the rapidly rising SO₄²⁻
20 concentration is considered as a crucial contributor to the eutrophication in shallow
21 lakes, however, the driving process and mechanism are still far from clear. In this study,
22 we constructed a series of microcosms with initial SO₄²⁻ concentrations of 0, 30, 60, 90,

23 120 and 150 mg/L to simulate the rapidly SO_4^{2-} increase of Lake Taihu subjected to
24 cyanobacteria blooms. Results showed that the sulfate reduction rate was stimulated by
25 the increase of initial SO_4^{2-} concentrations and cyanobacteria-derived organic matter,
26 with the maximal sulfate reduction rate of 39.68 mg/L·d in the treatment of 150 mg/L
27 SO_4^{2-} concentration. During the sulfate reduction, the produced maximal ΣS^{2-}
28 concentration in the overlying water and acid volatile sulfate (AVS) in the sediments
29 were 3.15 mg/L and 11.11 mg/kg, respectively, and both of them were positively
30 correlated with initial SO_4^{2-} concentrations ($R^2=0.97$; $R^2=0.92$). The increasing
31 abundance of sulfate reduction bacteria (SRB) was also linearly correlated with initial
32 SO_4^{2-} concentrations ($R^2=0.96$), ranging from 6.65×10^7 to 1.97×10^8 copies/g. However,
33 the Fe^{2+} concentrations displayed a negative correlation with initial SO_4^{2-}
34 concentrations, and the final Fe^{2+} concentrations were 9.68, 7.07, 6.5, 5.57, 4.42 and
35 3.46 mg/L, respectively. As a result, the released TP in the overlying water, to promote
36 the eutrophication, was up to 1.4 mg/L in the treatment of 150 mg/L SO_4^{2-} concentration.
37 Therefore, it is necessary to consider the effect of rapidly increasing SO_4^{2-}
38 concentrations on the release of endogenous phosphorus and the eutrophication in lakes.

39 **1.Introduction**

40 Nowadays, cyanobacteria bloom in eutrophic lakes has become one of the most
41 serious problems in freshwater lakes all over the world (Iwayama et al., 2017; Ho et al.,
42 2019). Phosphorus, as a necessary nutrient for biological growth, is considered to be
43 one of the main limiting factors of lake eutrophication (Ni et al., 2020). In recent years,
44 the input of exogenous phosphorus has been effectively controlled, while the release of

45 endogenous phosphorus is still an urgent problem in eutrophic lakes (Liu et al., 2018;
46 Guo et al., 2020). The release of endogenous phosphorus is affected by many factors,
47 such as wind and wave and the cyanobacteria decomposition (Xu et al., 2018; Zhao et
48 al., 2019). There are many forms of phosphorus in freshwater lake sediments, including
49 aluminum bound phosphorus (Al-P), iron bound phosphorus (Fe-P), etc. Among them,
50 Fe-P, formed under the condition of high dissolved oxygen (DO), is the most active
51 form of phosphorus in the sediments, which has a more obvious response to the change
52 of DO (Zhang et al., 2020). The accumulation and decay of cyanobacteria in eutrophic
53 lakes will change the physical and chemical environments of water body and form
54 anaerobic reduction conditions (Yan et al., 2017). This will facilitate the reduction of
55 iron oxides and lead to the desorption and release of Fe-P in sediments, resulting in the
56 increase of endogenous phosphorus release (Zhao et al., 2019).

57 Iron reduction plays an important role in natural ecosystems. It has been reported
58 that dissimilatory reduction of iron accounts for 22% of the total amount of organic
59 matter anaerobic mineralization in offshore areas (Thamdrup et al., 2004). According
60 to the classical theory, iron oxides or hydroxides can adsorb phosphorus in the water
61 and form Fe-P precipitation (Gunnars et al., 1997). In freshwater lakes, the lack of Fe(III)
62 content or the diagenesis of organic phosphorus may be the reason for the lack of
63 phosphorus in the overlying water. Therefore, the formation of iron oxides on the
64 surface of sediments is closely related to the phosphorus cycle process (Amirbahman
65 et al., 2003; Chen et al., 2014). The interaction between iron and phosphorus is reflected
66 in the effect of adsorption and desorption of Fe oxide on the P content in the overlying

67 water, since Fe-P is the main internal source of phosphorus (Wu et al., 2019). Iron
68 oxides can be used as both the source and destination of phosphorus in lake ecosystems
69 (Mort et al., 2010; Azam et al., 2014). In anaerobic reduction environments, iron
70 reduction can significantly promote the resolution of Fe-P. The Fe^{2+} generated by the
71 reaction can form FeS solid with soluble sulfide. In addition, free Fe^{3+} will combine
72 with humus to form stable complex, which further prevents the co-precipitation process
73 of phosphorus and iron oxides (Mort et al., 2010; Zhang et al., 2020). Therefore, iron
74 reduction process driven by cyanobacteria decomposition affects the circulation of
75 phosphorus in freshwater lakes.

76 Due to the SO_4^{2-} concentration in seawater reaching 28 mM, sulfate reduction
77 process with the participation of sulfate reduction bacteria (SRB) has received
78 considerable attention in the basic material cycle of marine biogeochemistry (Fike et
79 al., 2015; Pan et al., 2020). In freshwater lakes, the SO_4^{2-} concentration is less than 800
80 μM , which is generally considered insufficient for continuous sulfate reduction (Hansel
81 et al., 2015). However, in recent years, with the continuous input of exogenous sulfur,
82 the SO_4^{2-} concentration in freshwater lakes increases significantly and the degree of the
83 eutrophication and the SO_4^{2-} concentration show a positive correlation (Dierberg et al.,
84 2011; Yu et al., 2013). For instance, the SO_4^{2-} concentration in Lake Taihu, one of the
85 typical eutrophic lakes worldwide, has increased from 30 to 100 mg/L in the past 70
86 years and it will continue to rise in the future (Yu et al., 2013; Zhou et al., 2022). The
87 impact of sulfate reduction on the material cycle of lake ecosystems may be far beyond
88 our knowledge (Baldwin et al., 2012; Yu et al., 2013). On the other hand, it has been

89 reported that sulfate reduction process is one of the important ways of anaerobic
90 metabolism of organic matter in freshwater lakes, and $\sum S^{2-}$ produced by sulfate
91 reduction process can mediate the iron reduction process (Jorgensen et al., 2019; Zhang
92 et al., 2020). SRB mainly uses SO_4^{2-} as the electron acceptor to complete anaerobic
93 respiration, and the sulfur compounds produced by anaerobic metabolism are bound
94 with iron and so on, which are fixed in the sediments and form AVS on the surface of
95 sediments (Holmer et al., 2001; Chen et al., 2016). Therefore, with the input of
96 exogenous sulfur, sulfate reduction process produced $\sum S^{2-}$ will further promote iron
97 reduction in freshwater lakes.

98 In freshwater lakes, iron cycle affects the process of phosphorus cycle, and sulfur
99 cycle plays an important role in regulating iron cycle. Therefore, the cycle of iron, sulfur
100 and phosphorus in freshwater lakes is inseparable (Wu et al., 2019; Zhao et al., 2019).
101 Studies have shown that even when SO_4^{2-} content was as low as 20 mg/L, the anaerobic
102 metabolism of organic substrates was still dominated by sulfate reduction. Therefore,
103 sulfate reduction process plays an important role in the lacustrine biochemical cycle
104 (Hansel et al., 2015). In the absence of cyanobacteria, sulfate reduction doesn't occur
105 even if the SO_4^{2-} concentration is higher (Zhao et al., 2021). This is because the
106 accumulation and decomposition of cyanobacteria not only change the environment of
107 water body, but also release a large amount of organic matter, which provides the
108 necessary conditions for the circulation of iron, sulfur and phosphorus (Yan et al., 2017;
109 Melemdez-Pastor et al., 2019). Therefore, under the co-effect of the increase of SO_4^{2-}
110 and the cyanobacteria decomposition, the sulfate reduction process and the effect of

111 iron reduction process on endogenous phosphorus release from sediments need to be
112 further studied.

113 In this study, a series of different initial concentrations of SO_4^{2-} were set according
114 to the variation trend of SO_4^{2-} concentrations over the years and the possible rising trend
115 of eutrophic Lake Taihu. The effects of increased SO_4^{2-} concentration and cyanobacteria
116 bloom on sulfate reduction coupled with the microbial processes were investigated. The
117 dynamic changes of Fe^{2+} and Fe^{3+} concentrations during iron reduction were studied in
118 order to reveal the effect of sulfate reduction on iron reduction. In addition, the dynamic
119 changes of phosphorus in the overlying water and sediment were investigated. Finally,
120 the coupled sulfate, iron and phosphorus cyclic processes affected by the increasing
121 sulfate concentration and cyanobacteria bloom were also comprehensively analyzed for
122 elucidating the phosphorus release dynamics to tracking the hidden promoter of
123 cyanobacteria bloom in eutrophic lakes. The findings may be benefit for evaluating the
124 effect of sulfate reduction in freshwater lakes and its impact on the promotion of iron
125 reduction and the release of endogenous phosphorus.

126 **2. Materials and methods**

127 *2.1 Sample collection and preparation*

128 Lake Taihu (31°24' 40" N, 120°1' 3" E), one of the largest eutrophic shallow lakes
129 in China, with an average depth of 2.4 m and an area of 2340 m² (Mao et al., 2021). In
130 this study, samples of sediments and cyanobacteria were collected in July 2020.
131 [Sediments \(0-20 cm\) from the west shoreline of the lake \(31°24'45"N, 120°0'42"E\)](#)
132 [were collected using a gravity core sampler \(length of 150 cm and diameter of 20 cm\).](#)

133 Cyanobacteria was collected and concentrated by sieving water through a fine-mesh
134 plankton (250 mesh). All the sediment and cyanobacteria samples were stored in an
135 incubator with ice packs and delivered to the laboratory immediately. The sediment
136 samples were blended thoroughly, homogenized, and sieved (100 mesh) to the
137 polyethylene bag. The cyanobacteria samples were flushed and centrifuged at 1500
138 r/min for 5 min by a CT15RT versatile refrigerated centrifuge (China) and freeze
139 drying by Biosafer-10A. Different gradient sulfate concentrations were prepared from
140 the high purity water and Na₂SO₄.

141 *2.2 Set-up of incubation microcosms*

142 To simulate the dramatical SO₄²⁻ increase and cyanobacteria blooms of eutrophic
143 Lake Taihu, a series of microcosms were constructed in this study. According to the
144 ratio of surface sediments and the average water depth and the cyanobacteria
145 accumulation density of 2500 g/m² during the breakout of cyanobacteria blooms of
146 Taihu Lake, 100 g of sediment, 200 ml of water and 0.11 g of cyanobacteria powder
147 were added into each bottle (Zhang et al., 2020). Meanwhile, according to the change
148 trend of SO₄²⁻ concentrations in Taihu Lake over the years and the possibility of further
149 increase in the future (Yu et al., 2013), the SO₄²⁻ concentrations in six microcosm
150 systems were configured as: 30, 60, 90, 120, 150 mg/L, and a control without SO₄²⁻,
151 respectively. The microcosm system adopted anaerobic bottles (Φ 75 mm, length 180
152 mm, volume 500 ml) as the reaction device. There were three replicates in each SO₄²⁻
153 concentration experimental group. Each group was sampled 17 times on 1, 2, 3, 4, 5, 6,
154 7, 9, 11, 14, 18, 23, 28, 33, 38, 43 and 48 d. Totally, there were 306 anaerobic bottles,

155 and all the anaerobic bottles were placed in a biochemical incubator at a temperature of
156 25 °C. The water, gas and soil samples were collected by destructive sampling, that is,
157 at each sampling point, 18 anaerobic bottles were opened for testing, which ensured the
158 anaerobic environment and air pressure for other bottles. A part of sediment was used
159 for microbe determination and kept in a refrigerator at -80 °C, and the rest sediment and
160 other samples were kept at 0-4 °C for less than 24 h before analysis.

161 *2.3 Chemical analytical methods*

162 All water samples were filtered through 0.45µm Nylon filters. Dissolved total
163 phosphorus (DTP) was determined by colorimetry after digestion with $K_2S_2O_8+NaOH$,
164 and the ammonium molybdate and ascorbic acid were used as chromogenic agents
165 (Ebina et al., 1983). Water DO, oxidation and reduction potential (ORP) were measured
166 using calibrated probes (MP525, China) during destructive sampling. The SO_4^{2-} was
167 detected using the turbidimetric method with the stabilizer of $BaCl_2$ and gelatin
168 (Tabatabai et al., 1974), and the $\sum S^{2-}$ was detected by methylene blue (Cline et al.,
169 1969). Fe^{2+} and Fe^{3+} was determined by colorimetric (Phillips et al., 1987). The
170 sediment total phosphorus (TP) was extracted and determined by colorimetry (Ruban
171 et al., 2001). The schematic diagram of the method to test acid volatile sulfate (AVS)
172 was showed in Fig.S5, briefly, 5 g sediment was put into a 250 ml glass flask and inside
173 a small beaker with 15 ml of $ZnAc_2 \cdot 2H_2O$ and $NaAc \cdot 3H_2O$ was used to absorb H_2S gas.
174 The tube A was connected by N_2 and continue for 5 minutes, then closed valve. 2 ml
175 ascorbic acid solution was added to prevent S^{2-} oxidation, and then 15 ml (6 mol/L)
176 hydrochloric acid was added with the reaction at room temperature for 18 h. AVS was

177 determined by zinc cold diffusion method (Hsieh et al., 1997).

178 *2.4 Quantification of SRB in sediments*

179 In order to confirm the changes of sediment SRB in the microcosms, RT-QPCR
180 technologies were used to determine the cell copy numbers of MPA and SRB on 0,7
181 and 38 d in the sediments.

182 The sediment samples were collected and frozen at -80 °C in an ultra-low
183 temperature freezer. The E.Z.N.A. ®Soil DNA Kit (Omega Bio-Tek, Norcross, GA,
184 USA) was used to extract the total genomic DNA from each soil sample according to
185 the manufacturer's instructions. Nucleic acid quality and concentration were
186 determined by 1% agarose gel electrophoresis and NanoDrop 2000 UV
187 spectrophotometer (Thermo Scientific, USA), respectively.

188 SRB in sediments were quantified using the quantitative polymerase chain
189 reaction (qPCR) method. The qPCR with primer sets targeting DSR1F+ (5'-
190 ACSCACTGGAAGCACGGCGG-3') and DSR-R (5'-GTGGMRCCGTGCAKRTT
191 GG-3') were used for the SRB in this study. The q-PCR experiments were performed
192 on a ABI7300 q-PCR instrument (Applied Biosystems, USA) using ChamQ SYBR
193 Color qPCR Master Mix as the signal dye. Each 20 µL reaction mixture contained 2 µL
194 of the template DNA and 16.5 µL of ChamQ SYBR Color qPCR Master Mix. Standard
195 curves for each gene were obtained by the tenfold serial dilution of standard plasmids
196 containing the target functional gene. All operations were followed the MIQE
197 guidelines.

198 *2.5 Statistical analysis*

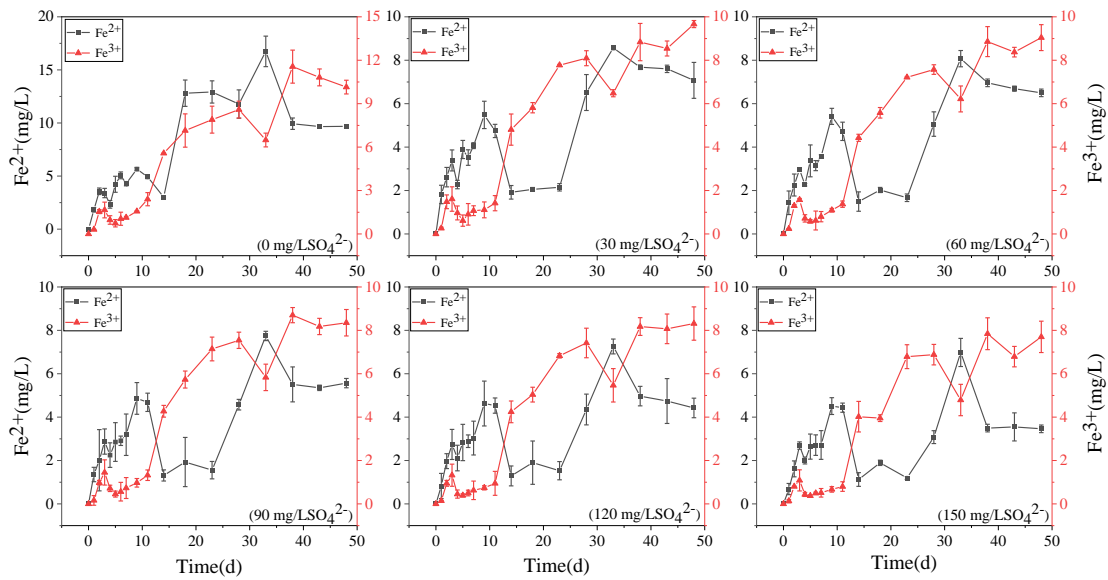
199 The Statistical Package of the Social Science 18.0 (SPSS 18.0) was used for
200 statistical analysis. The one-way analysis of variance (ANOVA) and correlation
201 analysis was carried out using bivariate correlations analysis.

202

203 **3.Results**

204 *3.1 Fe²⁺ and Fe³⁺ dynamics in overlying water*

205 The concentration variations of Fe²⁺ and Fe³⁺ in overlying water during the
206 incubation was presented in Fig.1. In the treatment without SO₄²⁻, they increased
207 continuously to 9.68 mg/L and 10.15 mg/L, respectively. The concentration of Fe³⁺ in
208 the remaining five treatments decreased at the beginning and then increased to keep
209 stable. The higher the initial sulfate concentration was, the lower the final Fe³⁺
210 concentration displayed. In the initial 150 mg/L SO₄²⁻ concentration treatment, the final
211 Fe³⁺ concentration was the lowest of 7.7 mg/L. The Fe²⁺ concentration in the five
212 treatments supplemented with SO₄²⁻ decreased significantly from 11 d to 23 d, and then
213 increased to a stable level. The final concentration of Fe²⁺ also showed a negative
214 correlation with the initial concentration of SO₄²⁻. In the initial 30 mg/L SO₄²⁻
215 concentration treatment, the final Fe²⁺ concentration was the highest of 7.07 mg/L.



216

217 Figure 1. The concentration variations of Fe^{2+} and Fe^{3+} in the water column during the
 218 incubation

219 3.2 SO_4^{2-} and $\sum\text{S}^{2-}$ dynamics in overlying water

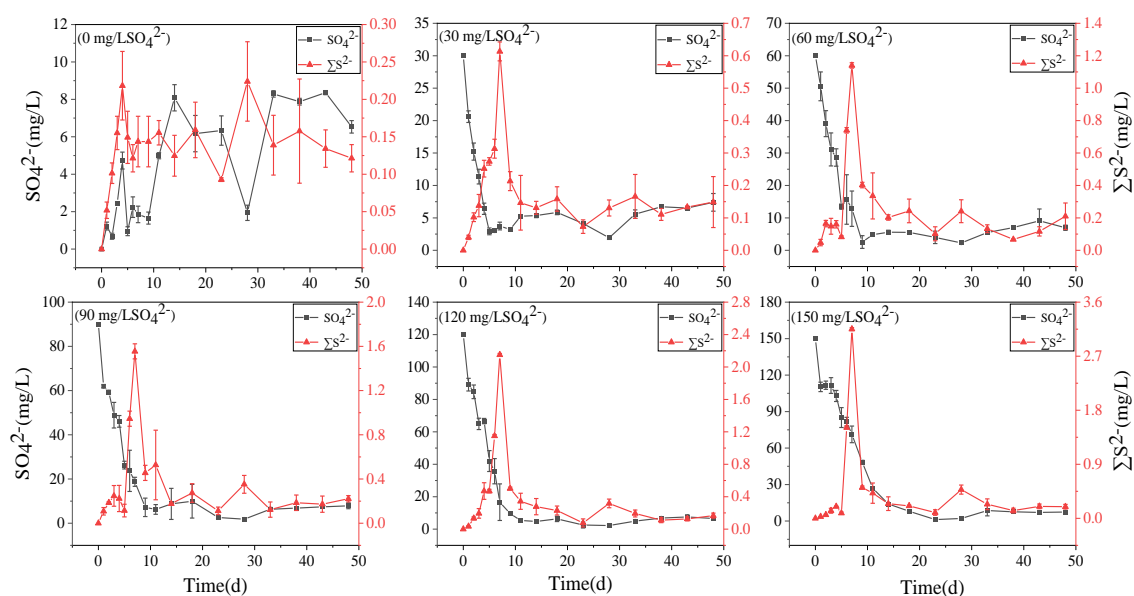
220 All treatments had obvious sulfate reduction reaction, and the concentration of
 221 SO_4^{2-} decreased greatly except for the treatment without adding SO_4^{2-} (Fig.2). The
 222 higher the initial sulfate concentration was, the faster the sulfate reduction rate in the
 223 initial stage exhibited (Tab.1). In the treatment with initial SO_4^{2-} concentration of 150
 224 mg/L, the sulphate reduction rate was 39.68 mg/L·d, while it was only 9.39 mg/L·d in
 225 the 30 mg/L SO_4^{2-} treatment. The sulfate reduction rate at the beginning of other
 226 treatments was also positively correlated with the initial SO_4^{2-} concentration.

227 The higher the initial SO_4^{2-} concentration was, the higher the maximum
 228 concentration of $\sum\text{S}^{2-}$ was. In the treatment with initial SO_4^{2-} concentration of 30 mg/L,
 229 the lowest concentration was 2.93 mg/L on the 5th day. However, the lowest SO_4^{2-}
 230 concentration appeared on the 23rd day was 1.18 mg/L in the treatment with initial
 231 SO_4^{2-} concentration of 150 mg/L. The maximum concentration of $\sum\text{S}^{2-}$ was positively

232 correlated with the initial SO_4^{2-} concentration. In the initial SO_4^{2-} concentrations of 30,
 233 60, 90, 120 and 150 mg/L SO_4^{2-} treatments, the highest ΣS^{2-} concentrations at 7 d were
 234 0.14, 0.61, 1.14, 1.55, 2.15, and 3.15 mg/L, respectively.

235 Table 1. Sulphate reduction rate in the water column of microcosms (mg/L·d)

SO_4^{2-} (mg/L) \ Time(d)	0	7	38
0	-	-	-
30	9.39	0.74	0.05
60	9.44	2.84	0.07
90	28.02	4.98	0.11
120	30.89	19.45	0.11
150	39.68	10.42	0.21



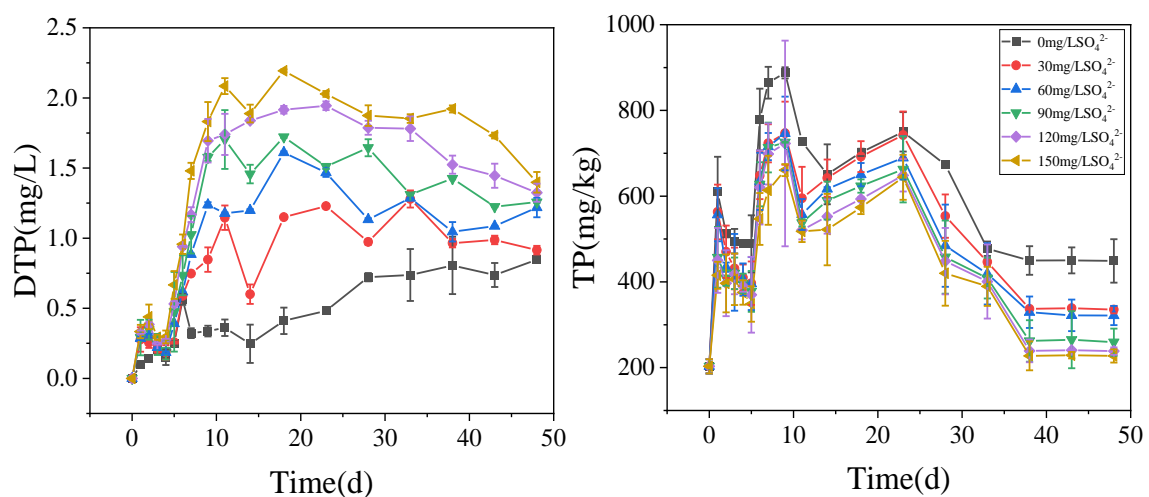
236
 237 Figure 2. The concentration variations of SO_4^{2-} and ΣS^{2-} in the water column during
 238 the incubation

239 3.3 TP dynamics in overlying water and sediments

240 The dynamics of DTP concentrations in overlying water during the incubation was
 241 presented (Fig.3 left). The concentrations of DTP in overlying water were positively
 242 correlated with the initial SO_4^{2-} . The higher the initial concentrations of SO_4^{2-} were, the

243 higher the concentrations of DTP in overlying water were. On 11 day, DTP in overlying
 244 water continued to rise and then kept stable. The highest DTP concentration was 2.08
 245 mg/L in the treatment with initial SO_4^{2-} concentration of 150 mg/L, while the highest
 246 DTP concentration was 0.36 mg/L in the treatment without SO_4^{2-} addition.

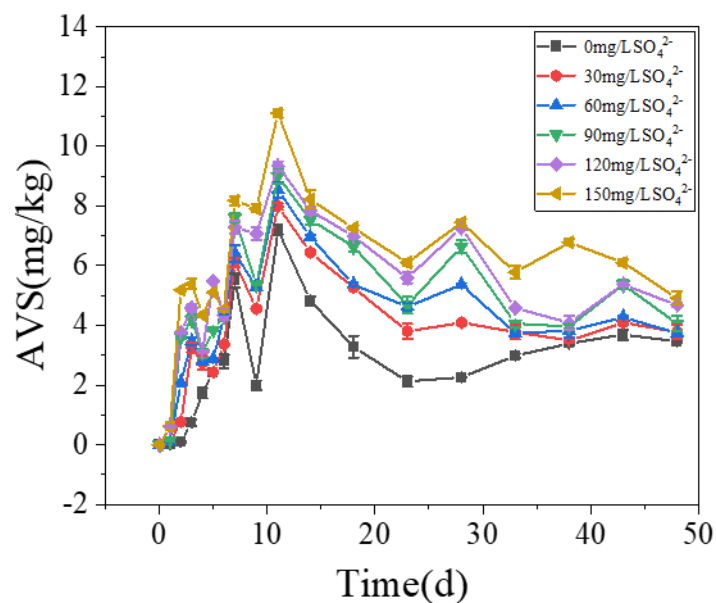
247 The concentrations of TP in the sediments increased significantly in all treatments
 248 with the cyanobacteria decomposition in the initial stage (Fig.3 right). Among of all
 249 treatments, on 9th day, the highest concentration of TP in the sediments was 887.69
 250 mg/kg in the treatment with initial SO_4^{2-} concentration of 0 mg/L. After 23 days, TP in
 251 the sediments decreased significantly and then stabilized. During cyanobacteria
 252 decomposition and sulfate reduction, the concentrations of TP in all treatments
 253 negatively correlated with the initial SO_4^{2-} concentration. The final TP concentration
 254 was 448.92, 335.32, 321.56, 259.32, 238.56 and 227.21 mg/kg, respectively in all
 255 treatments.



256
 257 Figure 3. The concentrations of TP in the overlying water (left) and sediments (right)
 258 during the incubation

259 *3.4 AVS dynamics in the sediments*

260 The concentrations of AVS in the sediments were positively correlated with the
 261 initial SO_4^{2-} concentrations. With the increase of TP in overlying water, the AVS in the
 262 sediments also increased steadily and reached the peak on the 11st days. In the treatment
 263 with initial SO_4^{2-} concentration of 0, 30, 60, 90, 120 and 150 mg/L, the highest
 264 concentration of AVS in the sediments were 7.21, 7.99, 8.54, 8.99, 9.34 and 11.11
 265 mg/kg, respectively.



266
 267 Figure 4. The concentration of AVS in the sediments during the incubation

268 3.5 SRB dynamics in the sediments

269 During the decomposition of cyanobacteria, the SRB abundance significantly
 270 increased compared with the initial stage ($P < 0.01$). In the initial stage, the SRB
 271 abundance was 1.09×10^8 copies/g and the final value was positively correlated with the
 272 initial SO_4^{2-} . On 7 d, SRB of all treatments showed a downward trend compared with
 273 the initial value, and there was no significant difference in SRB values between each
 274 treatment. On 38 d, except for the initial SO_4^{2-} concentrations of 0 and 30 mg/L, SRB
 275 increased significantly in other treatments.

276 Table 2. Copy numbers of the *dsrB* gene of SRB in the sediments during the incubation
 277 (copies/g)

Time SO ₄ ²⁻ (mg/L)	0 d	7 d	38 d
0	1.09×10 ⁸	5.81×10 ⁷	6.65×10 ⁷
30	1.09×10 ⁸	6.13×10 ⁷	7.71×10 ⁷
60	1.09×10 ⁸	7.61×10 ⁷	1.15×10 ⁸
90	1.09×10 ⁸	7.87×10 ⁷	1.31×10 ⁸
120	1.09×10 ⁸	7.99×10 ⁷	1.49×10 ⁸
150	1.09×10 ⁸	8.23×10 ⁷	1.91×10 ⁸

278 **4. Discussion**

279 It is generally acknowledged that climate warming and exogenous nutrient input
 280 are the important contributors to the occurrence of cyanobacteria blooms (Anneville et
 281 al., 2015; Yan et al., 2017). However, in this study, we found that the dramatically
 282 increasing SO₄²⁻ concentration in eutrophic lakes is also a non-negligible promoter for
 283 the self-sustaining of cyanobacteria blooms. In eutrophic lakes, the decomposition of
 284 cyanobacteria consumed DO in the water, and formed strong anaerobic reduction
 285 conditions (Fig.S1). Fe-P was desorbed to from free Fe³⁺, which was reduced to Fe²⁺ in
 286 anaerobic environments (Fig.1). Free Fe²⁺ combined with ΣS²⁻ which generated by
 287 sulfate reduction and eventually formed AVS fixed in the sediments (Fig.4), and
 288 phosphorus was released from the sediments (Fig.3). It has been reported that SRB and
 289 iron reduction bacteria (IRB) are the main microorganisms that drive sulfate reduction
 290 and iron reduction, respectively, and cyanobacteria decomposition promotes these
 291 microorganisms' growth (Wu et al., 2018). Consistent with these results, our findings
 292 also revealed that cyanobacteria released large amounts of organic matter to promote
 293 microbial growth during their decay and decomposition (Fig.S2, Tab. 2) and ultimately

294 promoted anaerobic reduction of sulfur and iron (Holmer et al., 2001). Therefore, with
295 increasing SO_4^{2-} concentrations in eutrophic lakes, the influence of sulfate reduction on
296 phosphorus release is worth further investigation.

297 Sulfur and iron in eutrophic lake sediments are directly related to iron and
298 phosphorus, and sulfur and phosphorus are also closely linked to bridges under the
299 action of iron (Zhang et al., 2020). With the increase of SO_4^{2-} concentration in eutrophic
300 lakes, the effect of sulfate reduction on phosphorus release from sediments may be more
301 important than previously recognized (Pester et al., 2012). Sulfate reduction driven by
302 SRB is an important organic metabolism pathway in natural systems. During the sulfate
303 reduction process, SO_4^{2-} is an electron acceptor and its concentration variation can
304 significantly affect the sulfate reduction rate (Holmer et al., 2001; Nakagawa et al.,
305 2012). SO_4^{2-} is reduced to $\sum\text{S}^{2-}$ by acquiring the electrons supplied by SRB oxidation,
306 and thus SRB plays an important role in sulfate reduction (Sela-Adler et al., 2017). The
307 increase of SO_4^{2-} concentration promotes the SRB abundance, as evidenced by a
308 positive correlation (Wu et al., 2018). In the case of increased SRB abundance (Tab. 2)
309 and increased SO_4^{2-} concentration, the sulfate reduction reaction was enhanced. The
310 SO_4^{2-} concentration in the overlying water decreased significantly accompanied by a
311 temporary increase in $\sum\text{S}^{2-}$ (Fig.2). The highest concentrations of $\sum\text{S}^{2-}$ also increased
312 with the initial SO_4^{2-} concentrations (Fig.5a). Interestingly, the $\sum\text{S}^{2-}$ decreased rapidly
313 after day 10 to almost zero at the end (Fig.2). This may result from the two keys: (a)
314 hydrogen sulfide overflows from the incubator; (b) sulfide migrates downward, and
315 combines with other substances in the sediment and is immobilized (Zhang et al., 2020).

316 In this study, TP in the overlying water has a significant positive correlation with the
317 initial SO_4^{2-} concentrations ($R^2 = 0.96$; Fig.3). The classical theory presumes that iron
318 reduction by IRB leads to the release of iron-bound phosphorus in the anaerobic layer
319 of sediments, and when the formed Fe^{2+} enters the aerobic water layer, it is oxidized by
320 Fe^{3+} and bound to phosphorus again (Roden et al., 2006; Chen et al., 2016). When the
321 sulfate reduction process mediates the iron reduction process, the released Fe^{2+}
322 combines with the product $\sum\text{S}^{2-}$ of sulfate reduction to form Fe-S, thus weakening the
323 reoxidation process of Fe^{2+} , and increasing the release of phosphorus (Mort et al., 2010;
324 Zhao et al., 2019). Therefore, with the increase of SO_4^{2-} concentrations in eutrophic
325 lakes, it significantly promoted the release of endogenous phosphorus from the
326 sediments.

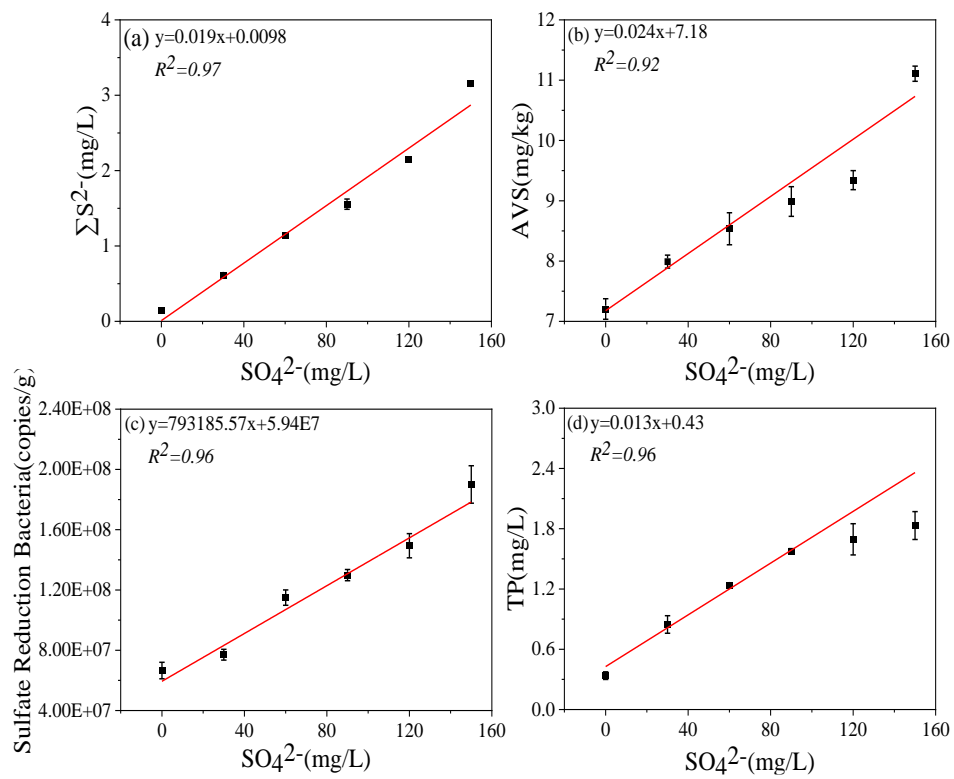
327 Although from a thermodynamic point of view, iron reduction should take
328 precedence over sulfur reduction (Han et al., 2015). However, due to chemical kinetics,
329 sulfur reduction occurs before iron reduction, resulting in the simultaneous appearance
330 of $\sum\text{S}^{2-}$ and iron oxides (Han et al., 2015; Hansel et al., 2015). This is consistent with
331 the concentration variation of iron and sulfur in this study (Fig.1-3). It has been reported
332 that iron cycles in the water body will produce an intense response to the accumulation
333 of sulfide, that is, sulfate reduction can promote iron reduction (Friedrich et al., 2014;
334 Zhang et al., 2020). $\sum\text{S}^{2-}$ is the final product of sulfate reduction, which is toxic to
335 microorganisms and easy to combine with heavy metals such as Fe^{2+} to form AVS in
336 lake sediments (Holmer et al., 2001). In this study, the concentration of AVS showed a
337 significant positive correlation with the initial concentration of SO_4^{2-} (Fig. 4, 5b), which

338 was consistent with the highest concentration of $\sum S^{2-}$ observed in the overlying water
339 (Fig. 2, 5c). The concentrations of Fe^{2+} and Fe^{3+} in the overlying water increased
340 significantly, and Fe^{2+} significantly decreased in the middle of the incubation (Fig. 1),
341 suggesting that Fe^{2+} reduced by sulfate can be combined with the product $\sum S^{2-}$ (Fig. 2).
342 These results consistent with the trend that AVS in the sediments reached a peak after
343 11 days and $\sum S^{2-}$ in the water decreased rapidly after 9 days and remained at a lower
344 concentration (Fig. 2, 3). The reason for this phenomenon may be the formation of Fe-
345 S compounds that is finally fixed in the sediments (Zhao et al., 2019).

346 The $\sum S^{2-}$ mediated iron chemical reduction may lead to more environmental
347 effects, such as phosphorus mobilization (Zhang et al., 2020). For instance, a previous
348 investigation on the lakes along the Yangtze River demonstrates that the effects of
349 endogenous phosphorus release is probably related to the increase of SO_4^{2-}
350 concentration (Chen et al., 2016). In this study, the concentration of Fe^{2+} in the
351 treatment without SO_4^{2-} continued to rise, and was up to the highest concentration
352 among all treatments (Fig. 1). In contrast, the concentrations of TP in the treatment
353 without SO_4^{2-} showed the lowest concentration among all treatments (Fig. 1, 5a). This
354 is caused by Fe^{2+} and Fe^{3+} recombining with phosphorus and being immobilized in the
355 sediments (Wu et al., 2019). In general, iron combines with phosphorus to form siderite
356 ($FePO_4 \cdot 2H_2O$) and blue iron ($Fe_3(PO_4)_2 \cdot 8H_2O$) and is bound to the sediments (Taylor
357 et al., 2011). However, when precipitation or reduction separates iron from iron
358 phosphate minerals, phosphorus bound to iron is released (Gu et al., 2016).

359 In order to further elucidate whether the increasing SO_4^{2-} concentrations in

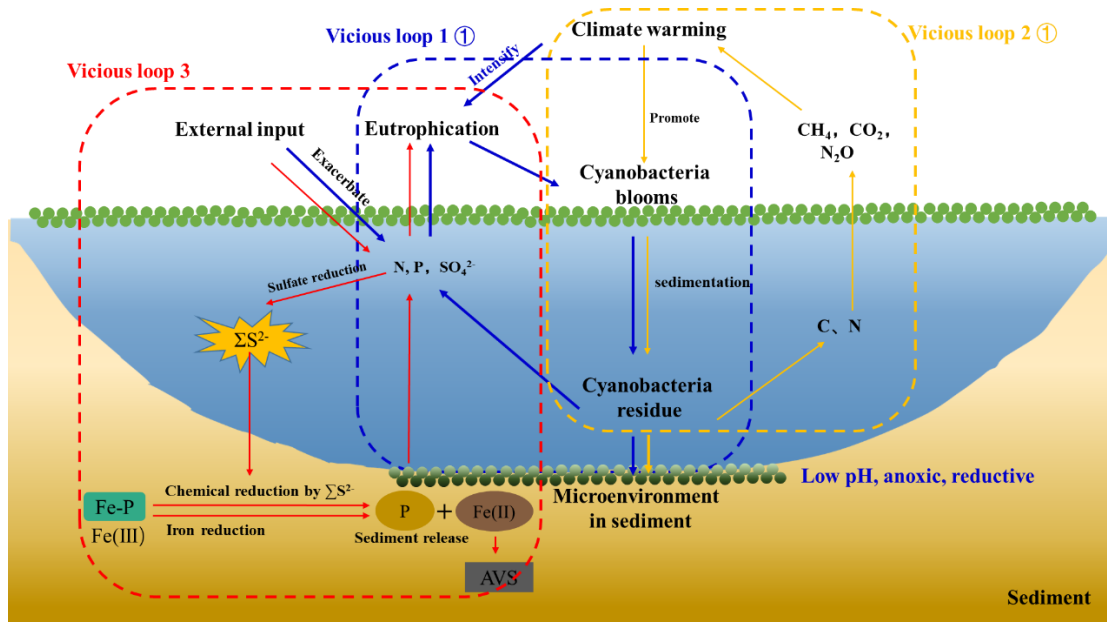
360 overlying water result in the self-sustaining of eutrophication in shallow lakes, a
361 conceptual diagram was put forward (Fig. 6). It has been accepted that exogenous
362 nutrient inputs and climate warming have positive effects on the breakout of
363 cyanobacteria blooms. With the continuous input of exogenous sulfur, the SO_4^{2-}
364 concentration in the lake water increases significantly. When cyanobacteria blooms
365 start to decay, the overlying water shifts from the aerobic state to the strong anaerobic
366 state, providing carbon source to promote the growth of microorganisms such as SRB.
367 The increasing SO_4^{2-} concentrations provide the electron for the sulfate reduction
368 process, resulting in the sulfate reduction and the release of a large amount of $\sum\text{S}^{2-}$. The
369 Fe^{2+} released from the iron reduction process is captured by $\sum\text{S}^{2-}$, and finally the
370 combination of iron and P was reduced, promoting the release of endogenous
371 phosphorus. Therefore, it is necessary to pay attention to the effect of enhanced sulfate
372 reduction on endogenous phosphorus release in eutrophic lakes.



373

374 Figure 5. Correlation of initial SO_4^{2-} concentrations with ΣS^{2-} (a), AVS(b), Sulfate-
 375 reducing bacteria (SRB) (c), TP (d) in the microcosm systems, respectively.

376



377

378 Figure 6. A simplified scheme of the relationship among climate warming, lake
 379 eutrophication and cyanobacteria blooms in eutrophic lakes. Under climate warming

380 scenarios, extreme abiotic and biotic conditions facilitated the breakout of
381 cyanobacteria blooms. After their collapse, the high amount of N, P, and C were
382 released into the overlying water and reacted with the eutrophication. Furthermore, a
383 large amount of CH₄ and CO₂ was produced and emitted to the atmosphere, contributing
384 to global warming of freshwater lakes (Yan et al. 2017). With the external sulfur input,
385 the concentration of SO₄²⁻ increased significantly and sulfate reduction was enhanced.
386 The cyanobacteria decomposition created an anaerobic reduction environment, which
387 will promote iron reduction and sulfate reduction. The free Fe³⁺ generated by Fe-P
388 desorption was reduced to Fe²⁺ and combined with ΣS²⁻ which produced by sulfate
389 reduction to form stable Fe-S in the sediments. Phosphorus was released from the
390 sediment into the overlying water. Therefore, there are three vicious loops between
391 cyanobacteria blooms occurrence, lake eutrophication and climate warming.

392

393 **5. Conclusion**

394 The dramatical increase of SO₄²⁻ concentration was up to more than 100 mg/L in
395 eutrophic lakes. There was a coupling relationship between sulfur, iron and phosphorus
396 cycles in lake ecosystems. Rapidly increasing sulfate concentration enhanced the
397 sulfate reduction to release of a large amount of ΣS²⁻ mediated by the increasing
398 abundance of SRB with the adequate organic source from the decay processes of
399 cyanobacteria blooms. The iron reduction, in positive with initial sulfate concentration,
400 occurred with the cyanobacteria decomposition. The Fe²⁺ released from the iron
401 reduction process was captured by ΣS²⁻, and finally the combination of iron and P was

402 reduced, promoting the release of endogenous phosphorus. Therefore, except for
403 climate warming and excessive nutrients, the increasing sulfate concentration is proved
404 to be another hidden promoter of eutrophication in shallow lakes.

405

406 **Author contributions**

407 Xu Xiaoguang: designed and led the study. Zhou Chuanqiao, Peng Yu, Chen Li,
408 Yu Miaotong, Muchun Zhou, Xu Runze, Lanqing Zhang, Siyuan Zhang: performed the
409 investigation and analysed the samples. Zhou Chuanqiao and Peng Yu: wrote the
410 original draft with major edits and inputs from Xu Xiaoguang, Zhang Limin and Wang
411 Guoxiang.

412

413 **Competing interests**

414 The authors declare that they have no known competing financial interests or
415 personal relationships that could have appeared to influence the work reported in this
416 paper.

417

418 **Acknowledgements**

419 This work was supported by the National Natural Science Foundation of China
420 (No.42077294, 41877336, 41971043), the Cooperation and Guidance Project of
421 Prospering Inner Mongolia through Science and Technology (No.2021CG0037), the
422 National Key Research and Development Program of China (No.2021YFC3200304),
423 the Guangxi Key Research and Development Program of China (No.2018AB36010).

424

425 **References**

426 Amirbahman, A., Pearce, A.R., Bouchard, R.J., Norton, S.A., Kahl, J.S.: Relationship
427 between hypolimnetic phosphorus and iron release from eleven lakes in Maine,
428 USA, *Biogeochemistry*, 65(3), 369-385, 10.1023/A:1026245914721, 2003.

429 Anneville, O., Domaizon, I., Kerimoglu, O., Rimet, F., Jacquet, S.: Blue-Green algae
430 in a “Greenhouse Century”? new insights from field data on climate change impacts
431 on cyanobacteria abundance, *Ecosystems*, 18(3), 441-458, 10.1007/s10021-014-
432 9837-6, 2015.

433 Azam, H.M., Finneran, K.T.: Fe(III) reduction-mediated phosphate removal as
434 vivianite ($\text{Fe}_3(\text{PO}_4)_2 \cdot 8\text{H}_2\text{O}$) in septic system wastewater, *Chemosphere*, 97, 1-9,
435 100.1016/j.chemosphere.2013.09.032, 2014.

436 Baldwin, D.S., Mitchell, A.: Impact of sulfate pollution on anaerobic biogeochemical
437 cycles in a wetland sediment, *Water Research*, 46(4), 965-974,
438 10.1016/j.watres.2011.11.065, 2012.

439 Chen, M., Li, X.H., He, Y.H., Song, N., Cai, H.Y., Wang, C.H., Li, Y.T., Chu, H.Y.,
440 Krumholz, L.R., Jing, H.L.: Increasing sulfate concentrations result in higher
441 sulfide production and phosphorous mobilization in a shallow eutrophic freshwater
442 lake, *Water Research*, 96, 94-104, 10.1016/j.watres.2016.03.030, 2016.

443 Chen, M., Ye, T.R., Krumholz, L.R., Jiang H.L.: Temperature and cyanobacteria bloom
444 biomass influence phosphorous cycling in eutrophic lake sediments, *Plos One*, 9(3),
445 e93130, 10.1371/journal.pone.0093130, 2014.

446 Cline, J.D.: Spectrophotometric determination of hydrogen sulfide in natural waters,
447 *Limnology and Oceanography*, 14, 454-458, 1969.

448 Dierberg, F.E., DeBusk, T.A., Larson, N.R., Kharbanda, M.D., Chan, N., Gabriel, M.C.:
449 Effect of sulfate amendments on mineralization and phosphorus release from South
450 Florida (USA) wetland soils under anaerobic conditions, *Soil Biology &*
451 *Biochemistry*, 43(1), 31-45, 10.1013/j.soilbio.2010.09.006, 2011.

452 Ebina, J., Tsutsui, T., Shirai, T.: Simultaneous determination of total nitrogen and total
453 phosphorus in water using peroxodisulfate oxidation, *Water Research*, 17(12),
454 1721-1726, 1983.

455 Fike, D.A., Bradley, A.S., Rose, C.V.: Rethinking the ancient sulfur cycle, *Annual*
456 *Review of Earth and Planetary Science*, 43, 593-622, 10.1146/annurev-warth-
457 060313-054802, 2015.

458 Friedrich, M.W., Finster, K.W.: How sulfur beats iron, *Science*, 344(6187), 974-975,
459 10.1126/science.1255442, 2014.

460 Gu, S., Qian, Y.G., Jiao, Y., Li, Q.M., Pinay, G., Gruau, G.: An innovative approach
461 for sequential extraction of phosphorus in sediments: Ferrous iron P as an
462 independent P fraction, *Water Research*, 103, 352-361,
463 10.1016/j.watres.2016.07.058, 2016.

464 Gunnars, A., Blomqvist, S.: Phosphate exchange across the sediment-water interface
465 when shifting from anoxic to oxic conditions an experimental comparison of
466 freshwater and brackish-marine systems, *Biogeochemistry*, 37(3), 203-226, 1997.

467 Guo, M.L., Li, X.L., Song, C.L., Liu, G.L., Zhou, Y.Y.: Photo-induced phosphate

468 release during sediment resuspension in shallow lakes: A potential positive
469 feedback mechanism of eutrophication, *Environmental Pollution*, 258, 113679,
470 10.1016/j.envpol.2019.113679, 2020.

471 Han, C., Ding, S.M., Yao, L., Shen, Q.S., Zhu, C.G., Wang, Y., Xu, D.: Dynamics of
472 phosphorus-iron-sulfur at the sediment-water interface influenced by algae blooms
473 decomposition, *Journal of Hazardous Materials*, 300, 329-337,
474 10.1016/j.jhazmat.2015.07.009, 2015.

475 Hansel, C.M., Lentini, C.J., Tang, Y.Z., Johnston, D.T., Wankel, S.D., Jardine, P.M.:
476 Dominance of sulfur-fueled iron oxide reduction in low-sulfate freshwater
477 sediments, *The ISME Journal*, 9(11), 2400-2412, 10.1038/ismej.2015.50, 2015.

478 Ho, J.C., Michalak, A.M., Pahlevan, N.: Widespread global increase in intense lake
479 phytoplankton blooms since the 1980s, *Nature* 574, 667-670, 10.1038/s41589-019-
480 1648-7, 2019.

481 Holmer, M., Storkholm, P.: Sulphate reduction and sulphur cycling in lake sediments:
482 a review, *Freshwater Biology*, 46, 431-451, 10.1046/j.1365-2427.2001.00687.x,
483 2001.

484 Hsieh, Y.P., Shieh, Y.N.: Analysis of reduced inorganic sulfur by diffusion methods:
485 improved apparatus and evaluation for sulfur isotopic studies, *Chemical Geology*,
486 137(3), 255-261, 1997.

487 Iwayama, A., Ogura, H., Hirama, Y., Chang, C.W., Hsieh, C.H., Kagami, M.:
488 Phytoplankton species abundance in Lake Inba (Japan) from 1986 to 2016,
489 *Ecological Research*, 32(6), 783-783, 10.1007/s11284-017-1482-z, 2017.

490 Jorgensen, B.B., Findlay, A.J., Pellerin, A.: The Biogeochemical sulfur cycle of Marine
491 sediments, *Frontiers in Microbiology*, 10, 849, 10.3389/fmicb.2019.00849, 2019.

492 Liu, Z.S., Zhang, Y., Han, F., Yan, P., Liu, B.Y., Zhou, Q.H., Min, F.L., He, F., Wu,
493 Z.B.: Investigation on the adsorption of phosphorus in all fractions from sediment
494 by modified maifanite, *Scientific Reports*, 8, 15619, 10.1038/s41598-018-34144-w,
495 2018.

496 Mao, Z.G., Gu, X.H., Cao, Y., Luo, J.H., Zeng, Q.F., Chen, H.H., Jeppesen, E.: How
497 does fish functional diversity respond to environmental changes in two large
498 shallow lakes? *Science of the total environment*, 753, 142158,
499 10.1016/j.scitotenv.2020.142158, 2021.

500 Mort, H.P., Slomp, C.P., Gustafsson, B.G., Andersen, T.J.: Phosphorus recycling and
501 burial in Baltic sea sediments with contrasting redox conditions, *Geochimica et*
502 *Cosmochimica Acta*, 74(4), 1350-1362, 10.1016/j.gca.2009.11.016, 2010.

503 Melemdez-Pastor, I., Isenstein, E.M., Navarro-Pedreno, J., Park, M.H.: Spatial
504 variability and temporal dynamics of cyanobacteria blooms and water quality
505 parameters in Missisquoi Bay (Lake Champlain), *Water Supply*, 19(5), 1500-1506,
506 10.2166/ws.2019.017, 2019.

507 Nakagawa, M., Ueno, Y., Hattori, S., Umemura, M., Yagi, A., Takai, K, Koba, K.,
508 Sasaki, Y., Makabe, A., Yoshida, N.: Seasonal change in microbial sulfur cycling
509 in monomictic Lake Fukami-ike, Japan, *Limnology and Oceanography*, 57(4), 974-
510 988, 10.4319/lo.2012.57.4.0974, 2012.

511 Ni, Z.K., Wang, S.R., Wu, Y., Pu, J.: Response of phosphorus fractionation in lake

512 sediments to anthropogenic activities in China, *Science of the Total Environment*,
513 699, 134242, 10.1016/j.scitotenv.2019.134242, 2020.

514 Pan, P., Guo, Z.R., Cai, Y., Liu, H.T., Wang, B., Wu, J.Y.: High-resolution imaging of
515 labile P&S in coastal sediment: Insight into the kinetics of P mobilization associated
516 with sulfate reduction, *Marine Chemistry*, 225, 103851, 10.1016/j.marchem.2020.
517 103851, 2020.

518 Pester, M., Knorr, K.H., Friedrich, M.W., Wagner, M., Loy, A.: Sulfate-reducing
519 microorganisms in wetlands-fameless actors in carbon cycling and climate change,
520 *Frontiers in Microbiology*, 3(72), 10.3389/fmicb.2012.00072, 2012.

521 Phillips, E.J.P., Lovley, D.R.: Determination of Fe(III) and Fe(II) in Oxalate Extracts
522 of Sediment, *Soil Science Society of America Journal*, 51: 938-941, 1987.

523 Roden, E.E.: Geochemical and microbiological controls on dissimilatory iron reduction,
524 *Comptes Rendus Geoscience*, 338(6-7), 456-467, 10.1016/j.crte.2006.04.009, 2006.

525 Ruban, V., Lopez-Sanchez, J.F., Pardo, P., Rauret, G., Muntau, H., Quevauviller, P.:
526 Harmonized protocol and certified reference material for the determination of
527 extractable contents of phosphorus in freshwater sediments-A synthesis of recent
528 works, *Fresenius J Anal Chem*, 370, 224-228, 10.1007/s002160100753, 2001.

529 Sela-Adler, M., Ronen, Z., Herut, B., Antler, G., Vigderovich, H., Eckert, W., Sivan,
530 O.: Co-existence of Methanogenesis and sulfate reduction with common substrates
531 in sulfate-rich estuarine sediments, *Frontiers in Microbiology*, 8(766),
532 10.3389/fmicb.2017.00766, 2017.

533 Tabatabai, M.: A rapid method for determination of sulfate in water samples,

534 Environmental, 7, 237-243, 1974.

535 Taylor, K.G., Konhauser, K.O.: Iron in Earth surface systems: a major player in
536 chemical and biological processes, Elements, 7(2), 83-87,
537 10.2113/gselements.7.2.83, 2011.

538 Thamdrup, B., Dalsgaard, T., Jensen, M.M., Petersen, J.: Anammox and the marine N
539 cycle, Geochimica et cosmochimica acta, 68(11), A325, 2004.

540 Wu, S.J., Zhao, Y.P., Chen, Y.Y., Dong, X.M., Wang, M.Y., Wang, G.X.: Sulfur
541 cycling in freshwater sediments: A cryptic driving force of iron deposition and
542 phosphorus mobilization, Science of the total environment, 657, 1294-1303,
543 10.1016/j.scitotenv. 2018.12.161, 2019.

544 Xu, G.H., Sun, Z.H., Fang, W.Y., Liu, J.J., Xu, X.B., Lv, C.X.: Release of phosphorus
545 from sediments under wave-induced liquefaction, Water Research, 144, 503-511,
546 10.1016 /j.watres.2018.07.038, 2018.

547 Yan, X.C., Xu, X.G., Wang, M.Y., Wang, G.X., Wu, S.J., Li, Z.C., Sun, H., Shi, A.,
548 Yang, Y.H.: Climate warming and cyanobacteria blooms: Looks at their
549 relationships from a new perspective, Water Research, 125, 449-457,
550 10.1016/j.watres.2017. 09.008, 2017.

551 Yu, T., Zhang, Y., Wu, F.C., Meng, W.: Six-Decade change in water chemistry of large
552 freshwater lake Taihu, China, Environmental Science and Technology, 47(16),
553 9093-9101, 10.1021/es401517h, 2013.

554 Zhang, S.Y., Zhao, Y.P., Zhou, C.Q., Duan, H.X., Wang, G.X.: Dynamic sulfur-iron
555 cycle promoted phosphorus mobilization in sediments driven by the algae

556 decomposition, *Ecotoxicology*, 30(8), 1662-1671, 10.1007/s10646-020-02316-y,
557 2020.

558 Zhao, Y.P., Wu, S.J., Yu, M.T., Zhang, Z.Q., Wang, X., Zhang, S.Y., Wang, G.X.:
559 Seasonal iron-sulfur interactions and the stimulated phosphorus mobilization in
560 freshwater lake sediments, *Science of the total environment*, 768, 144336,
561 10.1016/j.scitotenv.2020.144336, 2021.

562 Zhao, Y.P., Zhang, Z.Q., Wang, G.X., Li, X.J., Ma, J., Chen, S., Deng, H., Annalisa
563 O.H.: High sulfide production induced by algae decomposition and its potential
564 stimulation to phosphorus mobility in sediment, *Science of the total environment*,
565 650, 163-172, 10.1016/j.scitotenv.2018.09.010, 2019.

566 Zhou, C.Q., Peng, Y., Deng, Y., Yu, M.T., Chen, L., Zhang, L.Q., Xu, X.G., Zhao, F.J.,
567 Yan, Y., Wang, GX.: Increasing sulfate concentration and sedimentary decaying
568 cyanobacteria co-affect organic carbon mineralization in eutrophic lakes sediments,
569 *Science of the total environment*, 2022, 806, 151260, 10.1016/j.scitotenv.2021.
570 151260, 2022.